Supporting information: Histogram-free reweighting to estimate vapor-liquid coexistence properties of non-simulated force fields

Richard A. Messerly,[*,†] Mohammad S. Barhaghi,[‡] Jeffrey J. Potoff,[‡] and Michael R. Shirts[¶]

†*Thermodynamics Research Center, National Institute of Standards and Technology, Boulder, Colorado, 80305, United States*

‡*Department of Chemical Engineering and Materials Science, Wayne State University, Detroit, Michigan 48202, United States*

¶*Department of Chemical and Biological Engineering, University of Colorado, Boulder, Colorado, 80309, United States*

E-mail: richard.messerly@nist.gov

Table SI.I: Equilibrium (fixed) bond lengths (r_{eq}). CH_x and CH_y represent CH_3, $CH_2(sp^3)$, $CH(sp^3)$, or $C(sp^3)$ sites.

Bending sites	r_{eq} (nm)		
	TraPPE	MiPPE	NERD
CH_x-CH_y	0.154	0.154	0.154
C(sp)-CH_x	–	0.146	–
CH≡CH	–	0.121	–
C≡CH	–	0.121	–

Table SI.II: Equilibrium bond angles (θ_{eq}) and force constants (k_θ/k_{B}), where k_{B} is the Boltzmann constant. CH_x and CH_y represent CH_3, $CH_2(sp^3)$, $CH(sp^3)$, or $C(sp^3)$ sites.

Bending sites	θ_{eq} (degrees)			k_θ/k_{B} (K/rad^2)
	TraPPE	MiPPE	NERD	
CH_x-CH_2-CH_y	114.0	114.0	114.0	62500
CH_x-CH-CH_y	112.0	112.0	109.5	62500
CH_x-C-CH_y	109.5	109.5	109.5	62500
CH_x-CH_2-C(sp)	–	112	–	62500
CH_x-C(sp)≡CH	–	180	–	30800
CH_x-C(sp)≡C	–	180	–	30800

Table SI.III: Fourier constants (c_n/k_{B}) in units of K. CH_x and CH_y represent CH_3, $CH_2(sp^3)$, $CH(sp^3)$, or $C(sp^3)$ sites.

Torsion sites	c_0/k_{B}	c_1/k_{B}	c_2/k_{B}	c_3/k_{B}
CH_x-CH_2-CH_2-CH_y	0.0	355.03	-68.19	791.32
CH_x-CH_2-CH-CH_y	-251.06	428.73	-111.85	441.27
CH_x-CH_2-C-CH_y	0.0	0.0	0.0	461.29
CH_x-CH-CH-CH_y	-251.06	428.73	-111.85	441.27
CH_x-CH_2-CH_2-C(sp)	94.88	162.00	-205.40	980.40
CH_x-CH_2-C(sp)≡C(sp)	0	0	0	0
CH_x-CH_2-C(sp)≡CH(sp)	0	0	0	0
CH_x-C(sp)≡C(sp)-CH_y	0	0	0	0

Table SI.IV: State points simulated for 2-methylpropane with the TraPPE force field.

T (K)	μ (K)	L (nm)
350	-3120	3.0
380	-3120	3.0
405	-3117	3.0
380	-2980	3.0
350	-2880	3.0
320	-2790	3.0
290	-2705	3.0
260	-2645	3.0
230	-2600	3.0
200	-2570	3.0

Table SI.V: State points simulated for 2,2-dimethylpropane with the TraPPE force field.

T (K)	μ (K)	L (nm)
380	-3405	3.0
410	-3405	3.0
440	-3405	3.0
410	-3250	3.0
380	-3140	3.0
350	-3037	3.0
330	-2970	3.0
300	-2900	3.0
270	-2820	3.0

SI.I Bonded parameters

SI.II State Points

SI.III Tabulated GCMC-MBAR results

SI.III.1 Cyclohexane

SI.III.2 Branched alkanes

SI.III.3 Alkynes

SI.IV Optimal ψ values

Table SI.VI: State points simulated for 2,2-dimethylbutane with the TraPPE force field.

T (K)	μ (K)	L (nm)
420	-3860	3.5
450	-3860	3.5
480	-3860	3.5
450	-3719	3.5
420	-3600	3.5
400	-3524	3.5
380	-3450	3.5
360	-3368	3.5
340	-3288	3.5
310	-3280	3.5

Table SI.VII: State points simulated for 2,3-dimethylbutane with the TraPPE force field.

T (K)	μ (K)	L (nm)
440	-4015	3.0
470	-4015	3.0
500	-4011	3.0
470	-3845	3.0
440	-3735	3.0
410	-3635	3.0
380	-3555	3.0
350	-3480	3.0
320	-3415	3.0

Table SI.VIII: State points simulated for 3,3-dimethylhexane with the TraPPE force field.

T (K)	μ (K)	L (nm)
500	-4670	3.5
530	-4670	3.5
560	-4670	3.5
520	-4476	3.5
490	-4370	3.5
460	-4268	3.5
430	-4164	3.5
400	-4039	3.5
370	-3925	3.5

Table SI.IX: State points simulated for 3-methyl-3-ethylpentane with the TraPPE force field.

T (K)	μ (K)	L (nm)
500	-4785	4.0
550	-4785	4.0
580	-4785	4.0
550	-4636	4.0
520	-4520	4.0
490	-4400	4.0
460	-4280	4.0
430	-4160	4.0
410	-4080	4.0
390	-3990	4.0

Table SI.X: State points simulated for 2,3,4-trimethylpentane with the TraPPE force field.

T (K)	μ (K)	L (nm)
480	-4740	3.5
520	-4740	3.5
565	-4735	3.5
530	-4549	3.5
500	-4436	3.5
470	-4337	3.5
440	-4241	3.5
410	-4182	3.5
380	-4090	3.5
350	-4020	3.5

Table SI.XI: State points simulated for 2,2,4-trimethylpentane with the TraPPE force field.

T (K)	μ (K)	L (nm)
480	-4600	4.0
530	-4600	4.0
560	-4600	4.0
530	-4450	4.0
500	-4330	4.0
470	-4210	4.0
440	-4090	4.0
410	-3960	4.0
380	-3840	4.0

Table SI.XII: State points simulated for cyclohexane with the TraPPE force field.

T (K)	μ (K)	L (nm)
450	-4350	3.0
500	-4350	3.0
550	-4350	3.0
500	-4120	3.0
460	-3977	3.0
410	-3790	3.0
350	-3562	3.0

Table SI.XIII: State points simulated for cyclohexane with the $\lambda_{\mathrm{CH_2}}^{(1)} = 14$ force field.

T (K)	μ (K)	L (nm)
450	-4389	3.0
500	-4389	3.0
550	-4389	3.0
500	-4164	3.0
460	-4033	3.0
410	-3891	3.0
360	-3780	3.0

Table SI.XIV: State points simulated for cyclohexane with the $\lambda_{\mathrm{CH_2}}^{(1)} = 16$ force field.

T (K)	μ (K)	L (nm)
450	-4367	3.0
500	-4367	3.0
550	-4367	3.0
500	-4149	3.0
460	-4024	3.0
410	-3893	3.0
360	-3792	3.0

Table SI.XV: State points simulated for cyclohexane with the $\lambda_{\mathrm{CH_2}}^{(1)} = 18$ force field.

T (K)	μ (K)	L (nm)
450	-4370	3.0
500	-4370	3.0
550	-4370	3.0
500	-4158	3.0
460	-4037	3.0
410	-3912	3.0
360	-3825	3.0

Table SI.XVI: State points simulated for cyclohexane with the $\lambda_{\mathrm{CH_2}}^{(1)} = 20$ force field.

T (K)	μ (K)	L (nm)
450	-4386	3.0
500	-4386	3.0
550	-4386	3.0
500	-4178	3.0
460	-4062	3.0
410	-3946	3.0
360	-3866	3.0

Table SI.XVII: State points simulated for 2-methylpropane with the MiPPE-gen force field.

T (K)	μ (K)	L (nm)
350	-3150	3.0
380	-3150	3.0
410	-3145	3.0
380	-3010	3.0
350	-2910	3.0
320	-2830	3.0
290	-2760	3.0
260	-2700	3.0
230	-2670	3.0
200	-2640	3.0

Table SI.XVIII: State points simulated for 2,2-dimethylpropane with the MiPPE-gen force field.

T (K)	μ (K)	L (nm)
368	-3344	3.0
398	-3344	3.0
430	-3400	3.0
398	-3216	3.0
372	-3124	3.0
346	-3032	3.0
326	-2961	3.0
299	-2865	3.0
270	-2759	3.0

Table SI.XIX: State points simulated for 2,2-dimethylbutane with the MiPPE-gen force field.

T (K)	μ (K)	L (nm)
415	-3873	3.5
445	-3873	3.5
480	-3895	3.5
450	-3756	3.5
420	-3654	3.5
400	-3588	3.5
380	-3521	3.5
360	-3454	3.5
340	-3384	3.5
310	-3380	3.5

Table SI.XX: State points simulated for 2,3-dimethylbutane with the MiPPE-gen force field.

T (K)	μ (K)	L (nm)
440	-4010	3.0
470	-4010	3.0
500	-4009	3.0
470	-3860	3.0
440	-3760	3.0
410	-3670	3.0
380	-3600	3.0
350	-3530	3.0
320	-3480	3.0

Table SI.XXI: State points simulated for 2,3,4-trimethylpentane with the MiPPE-gen force field.

T (K)	μ (K)	L (nm)
480	-4720	3.5
520	-4720	3.5
565	-4713	3.5
530	-4540	3.5
500	-4360	3.5
470	-4355	3.5
440	-4275	3.5
410	-4205	3.5
380	-4165	3.5
350	-4115	3.5

Table SI.XXII: State points simulated for 2,2,4-trimethylpentane with the MiPPE-gen force field.

T (K)	μ (K)	L (nm)
470	-4570	4.0
520	-4570	4.0
550	-4570	4.0
520	-4420	4.0
490	-4300	4.0
460	-4170	4.0
430	-4050	4.0
400	-3920	4.0
370	-3790	4.0

Table SI.XXIII: GCMC-MBAR results for 2-methylpentane with the MiPPE-SL force field. Subscripts correspond to the 95% confidence interval computed with bootstrap re-sampling.

T^{sat} (K)	$\rho_{\mathrm{liq}}^{\mathrm{sat}}$ (kg/m^3)	$\rho_{\mathrm{vap}}^{\mathrm{sat}}$ (kg/m^3)	$P_{\mathrm{vap}}^{\mathrm{sat}}$ (MPa)	ΔH_{v} (kJ/mol)	$Z_{\mathrm{vap}}^{\mathrm{sat}}$
470	$422.20_{0.56}$	$76.7_{1.5}$	$20.68_{0.17}$	$14.14_{0.11}$	$0.595_{0.012}$
460	$444.71_{0.79}$	$61.2_{1.2}$	$17.61_{0.13}$	$16.06_{0.12}$	$0.649_{0.013}$
450	$464.38_{0.87}$	$49.31_{0.88}$	$14.918_{0.096}$	$17.71_{0.11}$	$0.697_{0.013}$
440	$481.69_{0.77}$	$40.17_{0.64}$	$12.557_{0.068}$	$19.106_{0.090}$	$0.736_{0.012}$
430	$497.34_{0.70}$	$32.86_{0.47}$	$10.491_{0.045}$	$20.318_{0.074}$	$0.770_{0.012}$
420	$511.89_{0.78}$	$26.86_{0.36}$	$8.690_{0.027}$	$21.408_{0.068}$	$0.798_{0.011}$
410	$525.69_{0.84}$	$21.87_{0.29}$	$7.130_{0.017}$	$22.412_{0.069}$	$0.824_{0.011}$
400	$538.82_{0.88}$	$17.70_{0.25}$	$5.788_{0.020}$	$23.344_{0.069}$	$0.848_{0.012}$
390	$551.23_{0.87}$	$14.21_{0.22}$	$4.645_{0.031}$	$24.207_{0.075}$	$0.869_{0.014}$
380	$562.89_{0.80}$	$11.30_{0.19}$	$3.681_{0.042}$	$25.004_{0.096}$	$0.888_{0.018}$
370	$573.96_{0.88}$	$8.90_{0.16}$	$2.878_{0.051}$	$25.75_{0.14}$	$0.906_{0.023}$
360	$584.8_{1.1}$	$6.92_{0.14}$	$2.215_{0.059}$	$26.46_{0.18}$	$0.922_{0.031}$
350	$595.6_{1.2}$	$5.31_{0.12}$	$1.677_{0.065}$	$27.15_{0.22}$	$0.935_{0.042}$
340	$606.3_{1.2}$	$4.01_{0.10}$	$1.245_{0.070}$	$27.83_{0.27}$	$0.947_{0.059}$
330	$616.4_{1.0}$	$2.969_{0.085}$	$0.906_{0.074}$	$28.45_{0.32}$	$0.958_{0.083}$
320	$625.82_{0.57}$	$2.156_{0.068}$	$0.644_{0.078}$	$29.04_{0.40}$	$0.97_{0.12}$

Table SI.XXIV: GCMC-MBAR results for 2-methylhexane with the MiPPE-SL force field. Subscripts correspond to the 95% confidence interval computed with bootstrap re-sampling.

T^{sat} (K)	$\rho_{\mathrm{liq}}^{\mathrm{sat}}$ (kg/m^3)	$\rho_{\mathrm{vap}}^{\mathrm{sat}}$ (kg/m^3)	$P_{\mathrm{vap}}^{\mathrm{sat}}$ (MPa)	ΔH_{v} (kJ/mol)	$Z_{\mathrm{vap}}^{\mathrm{sat}}$
510	$406.8_{3.4}$	$88.4_{2.0}$	$20.92_{0.11}$	$14.14_{0.12}$	$0.559_{0.013}$
500	$431.2_{2.2}$	$70.0_{1.6}$	$17.989_{0.052}$	$16.506_{0.085}$	$0.620_{0.014}$
490	$452.1_{1.2}$	$56.5_{1.0}$	$15.403_{0.041}$	$18.472_{0.088}$	$0.671_{0.013}$
480	$470.38_{0.73}$	$46.30_{0.50}$	$13.120_{0.056}$	$20.092_{0.065}$	$0.7116_{8.3e-3}$
470	$486.88_{0.50}$	$38.21_{0.17}$	$11.104_{0.062}$	$21.497_{0.034}$	$0.7453_{5.3e-3}$
460	$502.20_{0.37}$	$31.56_{0.16}$	$9.327_{0.058}$	$22.762_{0.022}$	$0.7744_{6.2e-3}$
450	$516.52_{0.39}$	$26.01_{0.17}$	$7.772_{0.050}$	$23.921_{0.024}$	$0.8003_{7.3e-3}$
440	$530.01_{0.34}$	$21.34_{0.15}$	$6.417_{0.043}$	$24.994_{0.024}$	$0.8236_{7.9e-3}$
430	$542.86_{0.37}$	$17.41_{0.14}$	$5.245_{0.039}$	$25.998_{0.031}$	$0.8444_{9.1e-3}$
420	$554.93_{0.46}$	$14.10_{0.13}$	$4.241_{0.037}$	$26.928_{0.041}$	$0.863_{0.011}$
410	$566.22_{0.43}$	$11.32_{0.14}$	$3.390_{0.036}$	$27.789_{0.046}$	$0.881_{0.014}$
400	$577.21_{0.43}$	$8.99_{0.14}$	$2.674_{0.037}$	$28.610_{0.060}$	$0.896_{0.019}$
390	$588.02_{0.38}$	$7.06_{0.15}$	$2.080_{0.039}$	$29.403_{0.089}$	$0.910_{0.026}$
380	$598.35_{0.22}$	$5.47_{0.16}$	$1.593_{0.044}$	$30.15_{0.14}$	$0.923_{0.037}$
370	$608.04_{0.19}$	$4.18_{0.16}$	$1.200_{0.050}$	$30.85_{0.20}$	$0.935_{0.053}$
360	$617.49_{0.27}$	$3.14_{0.16}$	$0.888_{0.057}$	$31.52_{0.28}$	$0.945_{0.077}$
350	$627.22_{0.26}$	$2.32_{0.15}$	$0.644_{0.065}$	$32.20_{0.39}$	$0.96_{0.11}$

Table SI.XXV: GCMC-MBAR results for 3-methylpentane with the MiPPE-SL force field. Subscripts correspond to the 95% confidence interval computed with bootstrap re-sampling.

T^{sat} (K)	$\rho_{\mathrm{liq}}^{\mathrm{sat}}$ (kg/m^3)	$\rho_{\mathrm{vap}}^{\mathrm{sat}}$ (kg/m^3)	$P_{\mathrm{vap}}^{\mathrm{sat}}$ (MPa)	ΔH_{v} (kJ/mol)	$Z_{\mathrm{vap}}^{\mathrm{sat}}$
480	$415.8_{1.5}$	84_{24}	$23.1_{2.4}$	$13.7_{1.3}$	$0.60_{0.18}$
470	$440.0_{2.3}$	67_{24}	$19.9_{1.4}$	$15.6_{1.7}$	$0.65_{0.23}$
460	$459.8_{2.5}$	55_{18}	$16.98_{0.59}$	$17.2_{1.6}$	$0.69_{0.22}$
450	$477.1_{1.9}$	$45.4_{7.6}$	$14.43_{0.12}$	$18.52_{0.94}$	$0.73_{0.12}$
440	$493.2_{1.2}$	$37.5_{1.5}$	$12.17_{0.14}$	$19.74_{0.27}$	$0.764_{0.032}$
430	$508.9_{1.4}$	$30.95_{0.38}$	$10.19_{0.15}$	$20.87_{0.11}$	$0.794_{0.015}$
420	$523.6_{1.1}$	$25.42_{0.36}$	$8.45_{0.14}$	$21.917_{0.094}$	$0.821_{0.018}$
410	$536.8_{1.4}$	$20.78_{0.32}$	$6.95_{0.14}$	$22.85_{0.12}$	$0.845_{0.021}$
400	$548.9_{1.7}$	$16.89_{0.24}$	$5.65_{0.13}$	$23.69_{0.15}$	$0.867_{0.023}$
390	$560.5_{1.5}$	$13.63_{0.21}$	$4.55_{0.12}$	$24.49_{0.13}$	$0.887_{0.027}$
380	$571.8_{1.2}$	$10.88_{0.20}$	$3.61_{0.10}$	$25.250_{0.099}$	$0.905_{0.031}$
370	$582.3_{1.1}$	$8.59_{0.18}$	$2.829_{0.089}$	$25.950_{0.093}$	$0.922_{0.035}$
360	$593.0_{1.1}$	$6.70_{0.16}$	$2.185_{0.077}$	$26.64_{0.12}$	$0.939_{0.040}$
350	$603.8_{1.0}$	$5.15_{0.14}$	$1.661_{0.067}$	$27.33_{0.14}$	$0.955_{0.047}$

Table SI.XXVI: GCMC-MBAR results for 3-methylhexane with the MiPPE-SL force field. Subscripts correspond to the 95% confidence interval computed with bootstrap re-sampling.

T^{sat} (K)	$\rho_{\mathrm{liq}}^{\mathrm{sat}}$ (kg/m^3)	$\rho_{\mathrm{vap}}^{\mathrm{sat}}$ (kg/m^3)	$P_{\mathrm{vap}}^{\mathrm{sat}}$ (MPa)	ΔH_{v} (kJ/mol)	$Z_{\mathrm{vap}}^{\mathrm{sat}}$
520	$398.4_{4.6}$	$98.1_{1.2}$	$23.07_{0.18}$	$13.25_{0.29}$	$0.5453_{7.9e-3}$
510	$426.2_{3.4}$	$77.3_{1.3}$	$19.96_{0.15}$	$15.86_{0.21}$	$0.610_{0.011}$
500	$449.0_{1.8}$	$62.6_{1.1}$	$17.20_{0.12}$	$17.92_{0.14}$	$0.662_{0.013}$
490	$467.85_{0.87}$	$51.64_{0.76}$	$14.74_{0.11}$	$19.56_{0.10}$	$0.702_{0.011}$
480	$484.12_{0.71}$	$42.82_{0.51}$	$12.562_{0.093}$	$20.963_{0.074}$	$0.737_{0.010}$
470	$498.93_{0.76}$	$35.54_{0.44}$	$10.638_{0.075}$	$22.215_{0.069}$	$0.768_{0.011}$
460	$512.9_{1.0}$	$29.46_{0.42}$	$8.944_{0.056}$	$23.366_{0.088}$	$0.796_{0.012}$
450	$526.2_{1.3}$	$24.34_{0.36}$	$7.463_{0.040}$	$24.442_{0.093}$	$0.821_{0.013}$
440	$539.09_{0.79}$	$20.03_{0.26}$	$6.171_{0.029}$	$25.454_{0.048}$	$0.844_{0.011}$
430	$551.25_{0.90}$	$16.38_{0.15}$	$5.055_{0.025}$	$26.397_{0.089}$	$0.8648_{8.9e-3}$
420	$563.0_{1.6}$	$13.302_{0.087}$	$4.097_{0.025}$	$27.29_{0.16}$	$0.8838_{7.9e-3}$
410	$574.5_{1.4}$	$10.70_{0.12}$	$3.283_{0.024}$	$28.15_{0.18}$	$0.902_{0.012}$
400	$585.3_{1.3}$	$8.53_{0.18}$	$2.598_{0.021}$	$28.96_{0.19}$	$0.918_{0.021}$
390	$595.7_{2.4}$	$6.72_{0.26}$	$2.028_{0.021}$	$29.72_{0.30}$	$0.933_{0.037}$
380	$605.9_{2.8}$	$5.23_{0.33}$	$1.560_{0.032}$	$30.45_{0.41}$	$0.947_{0.063}$
370	$615.4_{1.3}$	$4.01_{0.38}$	$1.181_{0.053}$	$31.13_{0.47}$	$0.96_{0.10}$
360	$624.92_{0.55}$	$3.04_{0.40}$	$0.878_{0.081}$	$31.78_{0.63}$	$0.97_{0.16}$

Table SI.XXVII: GCMC-MBAR results for 2,3-dimethylpentane with the MiPPE-SL force field. Subscripts correspond to the 95% confidence interval computed with bootstrap resampling.

T^{sat} (K)	$\rho_{\mathrm{liq}}^{\mathrm{sat}}$ (kg/m^3)	$\rho_{\mathrm{vap}}^{\mathrm{sat}}$ (kg/m^3)	$P_{\mathrm{vap}}^{\mathrm{sat}}$ (MPa)	ΔH_{v} (kJ/mol)	$Z_{\mathrm{vap}}^{\mathrm{sat}}$
510	$427.9_{1.6}$	81_{10}	$20.82_{0.91}$	$15.20_{0.53}$	$0.606_{0.081}$
500	$451.7_{1.0}$	$66.3_{9.6}$	$18.00_{0.57}$	$17.17_{0.70}$	$0.654_{0.097}$
490	$471.41_{0.86}$	$54.7_{7.1}$	$15.49_{0.28}$	$18.83_{0.70}$	$0.696_{0.091}$
480	$488.48_{0.89}$	$45.5_{4.0}$	$13.245_{0.092}$	$20.25_{0.54}$	$0.731_{0.064}$
470	$503.90_{0.73}$	$37.9_{1.7}$	$11.257_{0.050}$	$21.50_{0.32}$	$0.762_{0.035}$
460	$518.28_{0.52}$	$31.50_{0.62}$	$9.501_{0.072}$	$22.64_{0.14}$	$0.790_{0.017}$
450	$532.03_{0.63}$	$26.12_{0.25}$	$7.956_{0.080}$	$23.709_{0.054}$	$0.816_{0.011}$
440	$545.26_{0.62}$	$21.57_{0.18}$	$6.606_{0.080}$	$24.711_{0.037}$	$0.839_{0.012}$
430	$557.77_{0.54}$	$17.70_{0.16}$	$5.435_{0.075}$	$25.646_{0.038}$	$0.860_{0.014}$
420	$569.33_{0.53}$	$14.43_{0.15}$	$4.426_{0.070}$	$26.504_{0.037}$	$0.880_{0.016}$
410	$580.03_{0.59}$	$11.68_{0.14}$	$3.565_{0.063}$	$27.290_{0.040}$	$0.897_{0.019}$
400	$590.33_{0.66}$	$9.36_{0.13}$	$2.837_{0.057}$	$28.032_{0.047}$	$0.913_{0.022}$
390	$600.50_{0.61}$	$7.43_{0.11}$	$2.229_{0.052}$	$28.747_{0.057}$	$0.927_{0.026}$
380	$610.33_{0.59}$	$5.831_{0.094}$	$1.726_{0.048}$	$29.424_{0.079}$	$0.939_{0.030}$
370	$620.01_{0.64}$	$4.512_{0.077}$	$1.315_{0.046}$	$30.08_{0.11}$	$0.950_{0.037}$
360	$630.25_{0.55}$	$3.438_{0.066}$	$0.984_{0.045}$	$30.75_{0.14}$	$0.959_{0.048}$
350	$640.58_{0.49}$	$2.572_{0.058}$	$0.722_{0.046}$	$31.42_{0.20}$	$0.966_{0.065}$

Table SI.XXVIII: GCMC-MBAR results for 2,3-dimethylhexane with the MiPPE-SL force field. Subscripts correspond to the 95% confidence interval computed with bootstrap resampling.

T^{sat} (K)	$\rho_{\mathrm{liq}}^{\mathrm{sat}}$ (kg/m^3)	$\rho_{\mathrm{vap}}^{\mathrm{sat}}$ (kg/m^3)	$P_{\mathrm{vap}}^{\mathrm{sat}}$ (MPa)	ΔH_{v} (kJ/mol)	$Z_{\mathrm{vap}}^{\mathrm{sat}}$
540	$422.2_{1.1}$	$84.5_{3.7}$	$19.48_{0.48}$	$15.98_{0.12}$	$0.586_{0.029}$
530	$445.87_{0.82}$	$68.6_{3.6}$	$16.89_{0.36}$	$18.23_{0.22}$	$0.638_{0.036}$
520	$466.30_{0.66}$	$56.3_{3.0}$	$14.58_{0.24}$	$20.17_{0.26}$	$0.684_{0.038}$
510	$484.13_{0.59}$	$46.7_{2.1}$	$12.53_{0.15}$	$21.81_{0.23}$	$0.722_{0.034}$
500	$499.99_{0.52}$	$39.0_{1.4}$	$10.703_{0.092}$	$23.24_{0.18}$	$0.755_{0.027}$
490	$514.34_{0.48}$	$32.51_{0.80}$	$9.084_{0.054}$	$24.51_{0.13}$	$0.783_{0.020}$
480	$527.67_{0.54}$	$27.08_{0.47}$	$7.657_{0.032}$	$25.677_{0.096}$	$0.809_{0.014}$
470	$540.41_{0.64}$	$22.49_{0.30}$	$6.406_{0.019}$	$26.765_{0.082}$	$0.833_{0.012}$
460	$552.77_{0.76}$	$18.58_{0.23}$	$5.313_{0.015}$	$27.797_{0.085}$	$0.854_{0.011}$
450	$564.84_{0.87}$	$15.26_{0.22}$	$4.366_{0.018}$	$28.78_{0.11}$	$0.874_{0.013}$
440	$576.56_{0.95}$	$12.43_{0.23}$	$3.553_{0.025}$	$29.73_{0.14}$	$0.892_{0.017}$
430	$587.55_{0.97}$	$10.05_{0.23}$	$2.860_{0.034}$	$30.60_{0.18}$	$0.909_{0.023}$
420	$597.72_{0.83}$	$8.05_{0.21}$	$2.274_{0.044}$	$31.40_{0.21}$	$0.924_{0.030}$
410	$607.46_{0.53}$	$6.39_{0.18}$	$1.787_{0.053}$	$32.16_{0.22}$	$0.937_{0.038}$
400	$617.12_{0.48}$	$5.01_{0.14}$	$1.384_{0.061}$	$32.90_{0.24}$	$0.949_{0.050}$
390	$626.72_{0.62}$	$3.88_{0.10}$	$1.056_{0.067}$	$33.64_{0.28}$	$0.959_{0.066}$
380	$636.43_{0.54}$	$2.959_{0.070}$	$0.792_{0.071}$	$34.36_{0.35}$	$0.967_{0.090}$
370	$646.47_{0.59}$	$2.219_{0.049}$	$0.583_{0.072}$	$35.10_{0.46}$	$0.98_{0.12}$

Table SI.XXIX: GCMC-MBAR results for 2,4-dimethylhexane with the MiPPE-SL force field. Subscripts correspond to the 95% confidence interval computed with bootstrap re-sampling.

T^{sat} (K)	$\rho_{\mathrm{liq}}^{\mathrm{sat}}$ (kg/m^3)	$\rho_{\mathrm{vap}}^{\mathrm{sat}}$ (kg/m^3)	$P_{\mathrm{vap}}^{\mathrm{sat}}$ (MPa)	ΔH_{v} (kJ/mol)	$Z_{\mathrm{vap}}^{\mathrm{sat}}$
540	$406.0_{3.8}$	$97.8_{2.1}$	$20.90_{0.36}$	$14.21_{0.22}$	$0.543_{0.015}$
530	$430.3_{3.2}$	$78.1_{2.3}$	$18.10_{0.28}$	$16.71_{0.16}$	$0.601_{0.020}$
520	$452.1_{1.9}$	$63.1_{2.2}$	$15.62_{0.19}$	$18.90_{0.15}$	$0.654_{0.024}$
510	$470.9_{1.1}$	$51.8_{1.9}$	$13.42_{0.13}$	$20.72_{0.19}$	$0.698_{0.026}$
500	$487.5_{1.1}$	$42.9_{1.4}$	$11.472_{0.080}$	$22.26_{0.19}$	$0.734_{0.024}$
490	$502.5_{1.2}$	$35.72_{0.85}$	$9.745_{0.054}$	$23.60_{0.16}$	$0.765_{0.019}$
480	$516.3_{1.4}$	$29.69_{0.47}$	$8.222_{0.043}$	$24.83_{0.13}$	$0.793_{0.013}$
470	$529.5_{1.6}$	$24.62_{0.27}$	$6.886_{0.037}$	$25.96_{0.11}$	$0.8174_{9.9e-3}$
460	$542.1_{1.7}$	$20.34_{0.18}$	$5.720_{0.031}$	$27.026_{0.098}$	$0.8399_{8.6e-3}$
450	$554.3_{1.8}$	$16.71_{0.13}$	$4.708_{0.026}$	$28.031_{0.098}$	$0.8603_{8.3e-3}$
440	$566.1_{1.8}$	$13.63_{0.10}$	$3.836_{0.024}$	$28.98_{0.10}$	$0.8786_{8.6e-3}$
430	$577.4_{1.6}$	$11.03_{0.11}$	$3.092_{0.023}$	$29.89_{0.11}$	$0.895_{0.011}$
420	$588.1_{1.4}$	$8.85_{0.15}$	$2.463_{0.022}$	$30.73_{0.13}$	$0.910_{0.018}$
410	$598.1_{1.1}$	$7.02_{0.19}$	$1.937_{0.024}$	$31.51_{0.17}$	$0.924_{0.028}$
400	$607.97_{0.72}$	$5.51_{0.22}$	$1.503_{0.031}$	$32.27_{0.22}$	$0.937_{0.042}$
390	$617.69_{0.31}$	$4.27_{0.23}$	$1.148_{0.042}$	$33.01_{0.29}$	$0.947_{0.062}$
380	$627.04_{0.22}$	$3.26_{0.22}$	$0.862_{0.055}$	$33.71_{0.42}$	$0.957_{0.090}$
370	$635.81_{0.19}$	$2.45_{0.20}$	$0.636_{0.068}$	$34.36_{0.62}$	$0.97_{0.13}$
360	$644.04_{0.32}$	$1.80_{0.18}$	$0.460_{0.080}$	$34.97_{0.91}$	$0.97_{0.19}$

Table SI.XXX: GCMC-MBAR results for 3,4-dimethylhexane with the MiPPE-SL force field. Subscripts correspond to the 95% confidence interval computed with bootstrap re-sampling.

T^{sat} (K)	$\rho_{\mathrm{liq}}^{\mathrm{sat}}$ (kg/m^3)	$\rho_{\mathrm{vap}}^{\mathrm{sat}}$ (kg/m^3)	$P_{\mathrm{vap}}^{\mathrm{sat}}$ (MPa)	ΔH_{v} (kJ/mol)	$Z_{\mathrm{vap}}^{\mathrm{sat}}$
550	$416.97_{0.84}$	$91.7_{2.1}$	$21.00_{0.24}$	$15.29_{0.11}$	$0.572_{0.015}$
540	$441.75_{0.84}$	$75.2_{2.0}$	$18.28_{0.18}$	$17.53_{0.13}$	$0.619_{0.017}$
530	$462.97_{0.65}$	$61.9_{1.6}$	$15.84_{0.12}$	$19.50_{0.14}$	$0.664_{0.018}$
520	$481.27_{0.52}$	$51.4_{1.2}$	$13.670_{0.076}$	$21.20_{0.13}$	$0.703_{0.017}$
510	$497.59_{0.51}$	$42.88_{0.80}$	$11.732_{0.044}$	$22.68_{0.12}$	$0.737_{0.014}$
500	$512.45_{0.50}$	$35.87_{0.49}$	$10.010_{0.025}$	$23.994_{0.090}$	$0.767_{0.011}$
490	$526.21_{0.55}$	$30.00_{0.31}$	$8.485_{0.015}$	$25.192_{0.073}$	$0.7931_{8.3e-3}$
480	$539.20_{0.79}$	$25.02_{0.22}$	$7.142_{0.014}$	$26.302_{0.072}$	$0.8169_{7.4e-3}$
470	$551.6_{1.1}$	$20.79_{0.18}$	$5.963_{0.017}$	$27.341_{0.083}$	$0.8385_{7.6e-3}$
460	$563.5_{1.3}$	$17.18_{0.15}$	$4.936_{0.023}$	$28.319_{0.097}$	$0.8583_{8.7e-3}$
450	$574.7_{1.3}$	$14.10_{0.14}$	$4.050_{0.028}$	$29.24_{0.11}$	$0.877_{0.011}$
440	$585.4_{1.2}$	$11.49_{0.12}$	$3.287_{0.033}$	$30.09_{0.11}$	$0.893_{0.013}$
430	$595.6_{1.1}$	$9.29_{0.11}$	$2.642_{0.037}$	$30.90_{0.11}$	$0.909_{0.017}$
420	$605.36_{0.91}$	$7.437_{0.097}$	$2.097_{0.040}$	$31.66_{0.11}$	$0.922_{0.021}$
410	$614.74_{0.65}$	$5.893_{0.085}$	$1.644_{0.042}$	$32.38_{0.12}$	$0.935_{0.027}$
400	$624.02_{0.41}$	$4.615_{0.075}$	$1.271_{0.044}$	$33.08_{0.14}$	$0.946_{0.036}$
390	$633.41_{0.31}$	$3.566_{0.067}$	$0.967_{0.045}$	$33.78_{0.17}$	$0.955_{0.048}$
380	$642.95_{0.22}$	$2.715_{0.059}$	$0.724_{0.045}$	$34.48_{0.22}$	$0.964_{0.064}$
370	$652.67_{0.19}$	$2.032_{0.051}$	$0.531_{0.046}$	$35.18_{0.29}$	$0.970_{0.087}$

Table SI.XXXI: GCMC-MBAR results for 2,2,3-trimethylbutane with the MiPPE-SL force field. Subscripts correspond to the 95% confidence interval computed with bootstrap resampling.

T^{sat} (K)	$\rho_{\mathrm{liq}}^{\mathrm{sat}}$ (kg/m^3)	$\rho_{\mathrm{vap}}^{\mathrm{sat}}$ (kg/m^3)	$P_{\mathrm{vap}}^{\mathrm{sat}}$ (MPa)	ΔH_{v} (kJ/mol)	$Z_{\mathrm{vap}}^{\mathrm{sat}}$
520	$427.6_{2.7}$	$90.4_{3.4}$	$23.10_{0.41}$	$14.20_{0.20}$	$0.592_{0.025}$
510	$451.1_{1.5}$	$73.9_{3.6}$	$20.14_{0.30}$	$16.22_{0.27}$	$0.644_{0.033}$
500	$471.00_{0.92}$	$61.5_{2.9}$	$17.48_{0.20}$	$17.84_{0.29}$	$0.684_{0.033}$
490	$488.37_{0.82}$	$51.6_{1.9}$	$15.09_{0.14}$	$19.22_{0.23}$	$0.719_{0.027}$
480	$503.84_{0.76}$	$43.39_{0.99}$	$12.95_{0.11}$	$20.44_{0.15}$	$0.749_{0.018}$
470	$518.11_{0.61}$	$36.42_{0.54}$	$11.046_{0.087}$	$21.544_{0.083}$	$0.778_{0.013}$
460	$531.60_{0.50}$	$30.51_{0.45}$	$9.358_{0.068}$	$22.566_{0.064}$	$0.803_{0.013}$
450	$544.35_{0.55}$	$25.49_{0.41}$	$7.870_{0.049}$	$23.512_{0.070}$	$0.827_{0.014}$
440	$556.68_{0.54}$	$21.21_{0.32}$	$6.564_{0.032}$	$24.402_{0.069}$	$0.848_{0.014}$
430	$568.85_{0.50}$	$17.55_{0.23}$	$5.424_{0.020}$	$25.255_{0.062}$	$0.866_{0.012}$
420	$580.37_{0.55}$	$14.42_{0.15}$	$4.436_{0.014}$	$26.050_{0.058}$	$0.8826_{9.3e-3}$
410	$590.79_{0.86}$	$11.748_{0.088}$	$3.590_{0.014}$	$26.769_{0.064}$	$0.8982_{7.5e-3}$
400	$600.6_{1.0}$	$9.476_{0.069}$	$2.870_{0.014}$	$27.440_{0.077}$	$0.9126_{8.0e-3}$
390	$610.62_{0.83}$	$7.560_{0.096}$	$2.267_{0.013}$	$28.107_{0.086}$	$0.927_{0.013}$
380	$621.8_{1.5}$	$5.96_{0.14}$	$1.765_{0.014}$	$28.82_{0.16}$	$0.940_{0.023}$
370	$633.5_{2.1}$	$4.63_{0.17}$	$1.353_{0.019}$	$29.56_{0.26}$	$0.952_{0.038}$
360	$643.07_{0.71}$	$3.54_{0.20}$	$1.019_{0.029}$	$30.16_{0.26}$	$0.963_{0.060}$

Table SI.XXXII: GCMC-MBAR results for 2,2,3-trimethylpentane with the MiPPE-SL force field. Subscripts correspond to the 95% confidence interval computed with bootstrap resampling.

T^{sat} (K)	$\rho_{\mathrm{liq}}^{\mathrm{sat}}$ (kg/m^3)	$\rho_{\mathrm{vap}}^{\mathrm{sat}}$ (kg/m^3)	$P_{\mathrm{vap}}^{\mathrm{sat}}$ (MPa)	ΔH_{v} (kJ/mol)	$Z_{\mathrm{vap}}^{\mathrm{sat}}$
550	$424.5_{1.7}$	$94.6_{5.8}$	$22.04_{0.85}$	$14.90_{0.26}$	$0.582_{0.042}$
540	$446.63_{0.90}$	$77.5_{4.4}$	$19.31_{0.70}$	$17.04_{0.27}$	$0.634_{0.043}$
530	$466.95_{0.61}$	$64.6_{2.9}$	$16.85_{0.58}$	$18.86_{0.22}$	$0.676_{0.039}$
520	$485.81_{0.76}$	$54.4_{1.9}$	$14.63_{0.50}$	$20.45_{0.13}$	$0.711_{0.035}$
510	$502.62_{0.63}$	$45.9_{1.6}$	$12.63_{0.44}$	$21.840_{0.082}$	$0.742_{0.037}$
500	$517.03_{0.59}$	$38.7_{1.7}$	$10.84_{0.37}$	$23.05_{0.11}$	$0.770_{0.043}$
490	$529.98_{0.76}$	$32.6_{1.9}$	$9.25_{0.29}$	$24.14_{0.18}$	$0.795_{0.053}$
480	$542.7_{1.0}$	$27.4_{1.8}$	$7.84_{0.21}$	$25.18_{0.25}$	$0.818_{0.059}$
470	$555.2_{1.2}$	$23.0_{1.6}$	$6.59_{0.13}$	$26.17_{0.29}$	$0.840_{0.059}$
460	$566.7_{1.3}$	$19.1_{1.2}$	$5.500_{0.068}$	$27.09_{0.30}$	$0.860_{0.054}$
450	$577.6_{1.2}$	$15.82_{0.81}$	$4.550_{0.027}$	$27.94_{0.29}$	$0.878_{0.045}$
440	$588.5_{3.8}$	$13.0_{1.5}$	4_{13}	$28.8_{7.3}$	$0.9_{3.1}$
430	$599.6_{2.4}$	$10.61_{0.31}$	$3.023_{0.035}$	$29.58_{0.30}$	$0.910_{0.029}$
420	$610.1_{2.1}$	$8.58_{0.19}$	$2.423_{0.044}$	$30.34_{0.26}$	$0.923_{0.026}$
410	$619.5_{1.4}$	$6.88_{0.12}$	$1.918_{0.049}$	$31.02_{0.22}$	$0.935_{0.029}$
400	$628.4_{1.5}$	$5.447_{0.098}$	$1.498_{0.051}$	$31.66_{0.24}$	$0.945_{0.036}$
380	$645.33_{0.68}$	$3.285_{0.097}$	$0.874_{0.051}$	$32.86_{0.25}$	$0.961_{0.062}$

Table SI.XXXIII: GCMC-MBAR results for 2,2,4-trimethylpentane with the MiPPE-SL force field. Subscripts correspond to the 95% confidence interval computed with bootstrap re-sampling.

T^{sat} (K)	$\rho_{\mathrm{liq}}^{\mathrm{sat}}$ (kg/m^3)	$\rho_{\mathrm{vap}}^{\mathrm{sat}}$ (kg/m^3)	$P_{\mathrm{vap}}^{\mathrm{sat}}$ (MPa)	ΔH_{v} (kJ/mol)	$Z_{\mathrm{vap}}^{\mathrm{sat}}$
530	$400.9_{2.2}$	$97.9_{4.8}$	$21.20_{0.38}$	$13.58_{0.32}$	$0.561_{0.029}$
520	$427.5_{1.3}$	$79.4_{3.2}$	$18.44_{0.28}$	$15.89_{0.27}$	$0.614_{0.027}$
510	$448.78_{0.77}$	$65.1_{1.8}$	$15.97_{0.21}$	$17.79_{0.18}$	$0.661_{0.020}$
500	$466.83_{0.75}$	$53.9_{1.1}$	$13.78_{0.18}$	$19.40_{0.13}$	$0.702_{0.017}$
490	$483.78_{0.81}$	$44.87_{0.89}$	$11.82_{0.15}$	$20.85_{0.12}$	$0.739_{0.017}$
480	$499.84_{0.70}$	$37.41_{0.89}$	$10.09_{0.12}$	$22.18_{0.12}$	$0.772_{0.020}$
470	$514.41_{0.57}$	$31.21_{0.86}$	$8.545_{0.083}$	$23.38_{0.13}$	$0.800_{0.023}$
460	$527.62_{0.53}$	$26.00_{0.75}$	$7.187_{0.053}$	$24.45_{0.13}$	$0.826_{0.025}$
450	$539.75_{0.68}$	$21.58_{0.59}$	$5.995_{0.030}$	$25.42_{0.12}$	$0.848_{0.024}$
440	$551.12_{0.66}$	$17.82_{0.43}$	$4.958_{0.022}$	$26.32_{0.12}$	$0.869_{0.021}$
430	$562.67_{0.50}$	$14.62_{0.31}$	$4.062_{0.027}$	$27.21_{0.13}$	$0.888_{0.020}$
420	$574.59_{0.49}$	$11.89_{0.25}$	$3.292_{0.035}$	$28.09_{0.13}$	$0.906_{0.021}$
410	$585.04_{0.41}$	$9.58_{0.25}$	$2.637_{0.042}$	$28.86_{0.15}$	$0.922_{0.028}$
400	$594.23_{0.30}$	$7.66_{0.27}$	$2.087_{0.051}$	$29.54_{0.20}$	$0.936_{0.040}$
390	$604.33_{0.26}$	$6.05_{0.29}$	$1.630_{0.063}$	$30.26_{0.28}$	$0.949_{0.058}$
380	$615.43_{0.23}$	$4.72_{0.30}$	$1.252_{0.077}$	$31.01_{0.41}$	$0.958_{0.084}$
370	$625.27_{0.23}$	$3.63_{0.29}$	$0.946_{0.092}$	$31.68_{0.58}$	$0.97_{0.12}$

Table SI.XXXIV: GCMC-MBAR results for 2,3,3-trimethylpentane with the MiPPE-SL force field. Subscripts correspond to the 95% confidence interval computed with bootstrap re-sampling.

T^{sat} (K)	$\rho_{\mathrm{liq}}^{\mathrm{sat}}$ (kg/m^3)	$\rho_{\mathrm{vap}}^{\mathrm{sat}}$ (kg/m^3)	$P_{\mathrm{vap}}^{\mathrm{sat}}$ (MPa)	ΔH_{v} (kJ/mol)	$Z_{\mathrm{vap}}^{\mathrm{sat}}$
560	$426.5_{9.5}$	$98.7_{1.6}$	$23.04_{0.24}$	$14.76_{0.51}$	$0.573_{0.011}$
550	$452.4_{5.9}$	$80.7_{1.4}$	$20.23_{0.20}$	$17.10_{0.29}$	$0.626_{0.013}$
540	$473.3_{2.0}$	$67.2_{1.1}$	$17.69_{0.18}$	$18.98_{0.12}$	$0.670_{0.013}$
530	$490.60_{0.59}$	$56.53_{0.74}$	$15.40_{0.16}$	$20.523_{0.065}$	$0.706_{0.012}$
520	$505.89_{0.92}$	$47.80_{0.63}$	$13.35_{0.14}$	$21.863_{0.043}$	$0.738_{0.012}$
510	$520.2_{1.1}$	$40.46_{0.65}$	$11.51_{0.12}$	$23.086_{0.038}$	$0.766_{0.014}$
500	$534.1_{1.0}$	$34.21_{0.66}$	$9.866_{0.088}$	$24.232_{0.057}$	$0.792_{0.017}$
490	$546.97_{0.93}$	$28.87_{0.60}$	$8.402_{0.063}$	$25.283_{0.071}$	$0.816_{0.018}$
480	$558.82_{0.80}$	$24.29_{0.47}$	$7.108_{0.044}$	$26.241_{0.071}$	$0.837_{0.017}$
470	$570.25_{0.87}$	$20.36_{0.30}$	$5.967_{0.036}$	$27.143_{0.070}$	$0.857_{0.014}$
460	$581.5_{1.1}$	$16.96_{0.17}$	$4.969_{0.037}$	$28.007_{0.066}$	$0.875_{0.011}$
450	$592.0_{1.0}$	$14.04_{0.13}$	$4.101_{0.041}$	$28.816_{0.071}$	$0.892_{0.012}$
440	$602.0_{1.1}$	$11.53_{0.15}$	$3.353_{0.046}$	$29.578_{0.085}$	$0.908_{0.017}$
430	$612.3_{1.6}$	$9.39_{0.16}$	$2.714_{0.052}$	$30.34_{0.10}$	$0.924_{0.024}$
420	$622.8_{1.6}$	$7.58_{0.16}$	$2.171_{0.058}$	$31.10_{0.13}$	$0.937_{0.032}$
410	$632.87_{0.75}$	$6.05_{0.16}$	$1.716_{0.064}$	$31.82_{0.20}$	$0.950_{0.044}$
400	$642.39_{0.29}$	$4.78_{0.17}$	$1.338_{0.070}$	$32.50_{0.28}$	$0.961_{0.061}$
390	$651.59_{0.31}$	$3.73_{0.18}$	$1.028_{0.075}$	$33.14_{0.37}$	$0.971_{0.085}$

Table SI.XXXV: GCMC-MBAR results for ethyne with the MiPPE force field. Subscripts correspond to the 95% confidence interval computed with bootstrap re-sampling.

T^{sat} (K)	$\rho_{\mathrm{liq}}^{\mathrm{sat}}$ (kg/m^3)	$\rho_{\mathrm{vap}}^{\mathrm{sat}}$ (kg/m^3)	$P_{\mathrm{vap}}^{\mathrm{sat}}$ (MPa)	ΔH_{v} (kJ/mol)	$Z_{\mathrm{vap}}^{\mathrm{sat}}$
290	$421.3_{3.5}$	$69.7_{3.3}$	$40.83_{0.20}$	$8.80_{0.21}$	$0.632_{0.030}$
280	$450.7_{1.9}$	$50.69_{0.91}$	$31.96_{0.26}$	$10.27_{0.12}$	$0.705_{0.014}$
270	$474.9_{3.0}$	$37.66_{0.39}$	$24.65_{0.24}$	$11.390_{0.086}$	$0.759_{0.011}$
260	$497.3_{1.1}$	$27.95_{0.53}$	$18.65_{0.17}$	$12.361_{0.034}$	$0.804_{0.017}$
250	$517.91_{0.59}$	$20.53_{0.34}$	$13.78_{0.12}$	$13.214_{0.042}$	$0.841_{0.016}$
240	$536.87_{0.67}$	$14.82_{0.12}$	$9.92_{0.10}$	$13.975_{0.028}$	$0.874_{0.011}$
230	$554.12_{0.54}$	$10.447_{0.095}$	$6.925_{0.089}$	$14.649_{0.037}$	$0.903_{0.014}$
220	$570.90_{0.53}$	$7.155_{0.097}$	$4.667_{0.082}$	$15.283_{0.049}$	$0.929_{0.021}$

Table SI.XXXVI: GCMC-MBAR results for propyne with the MiPPE force field. Subscripts correspond to the 95% confidence interval computed with bootstrap re-sampling.

T^{sat} (K)	$\rho_{\mathrm{liq}}^{\mathrm{sat}}$ (kg/m^3)	$\rho_{\mathrm{vap}}^{\mathrm{sat}}$ (kg/m^3)	$P_{\mathrm{vap}}^{\mathrm{sat}}$ (MPa)	ΔH_{v} (kJ/mol)	$Z_{\mathrm{vap}}^{\mathrm{sat}}$
380	$441.0_{7.9}$	$82.2_{3.1}$	$38.39_{0.90}$	$10.96_{0.34}$	$0.592_{0.026}$
370	$472.7_{5.0}$	$62.7_{2.7}$	$31.64_{0.73}$	$12.83_{0.31}$	$0.657_{0.033}$
360	$498.3_{2.8}$	$48.6_{1.9}$	$25.84_{0.57}$	$14.34_{0.24}$	$0.711_{0.032}$
350	$520.1_{2.4}$	$38.1_{1.3}$	$20.88_{0.45}$	$15.58_{0.19}$	$0.754_{0.030}$
340	$539.4_{2.1}$	$29.88_{0.90}$	$16.67_{0.35}$	$16.65_{0.15}$	$0.791_{0.029}$
330	$556.6_{1.4}$	$23.31_{0.72}$	$13.13_{0.27}$	$17.58_{0.11}$	$0.822_{0.031}$
320	$572.1_{1.3}$	$18.02_{0.60}$	$10.18_{0.19}$	$18.41_{0.11}$	$0.850_{0.032}$
310	$587.6_{1.3}$	$13.76_{0.47}$	$7.76_{0.12}$	$19.20_{0.12}$	$0.876_{0.033}$
300	$603.3_{1.5}$	$10.35_{0.32}$	$5.799_{0.068}$	$19.97_{0.13}$	$0.900_{0.030}$
290	$617.9_{2.2}$	$7.65_{0.20}$	$4.240_{0.040}$	$20.67_{0.15}$	$0.921_{0.025}$

Table SI.XXXVII: GCMC-MBAR results for 1-butyne with the MiPPE force field. Subscripts correspond to the 95% confidence interval computed with bootstrap re-sampling.

T^{sat} (K)	$\rho_{\mathrm{liq}}^{\mathrm{sat}}$ (kg/m^3)	$\rho_{\mathrm{vap}}^{\mathrm{sat}}$ (kg/m^3)	$P_{\mathrm{vap}}^{\mathrm{sat}}$ (MPa)	ΔH_{v} (kJ/mol)	$Z_{\mathrm{vap}}^{\mathrm{sat}}$
410	$445.1_{5.3}$	76_{12}	$29.5_{1.0}$	$12.82_{0.72}$	$0.620_{0.097}$
400	$472.3_{3.4}$	$59.2_{6.8}$	$24.64_{0.50}$	$14.61_{0.60}$	$0.677_{0.079}$
390	$495.0_{2.6}$	$47.1_{2.3}$	$20.38_{0.30}$	$16.08_{0.32}$	$0.722_{0.037}$
380	$515.5_{2.0}$	$37.54_{0.86}$	$16.69_{0.23}$	$17.37_{0.16}$	$0.761_{0.020}$
370	$534.5_{1.3}$	$29.90_{0.70}$	$13.51_{0.18}$	$18.53_{0.13}$	$0.795_{0.021}$
360	$552.0_{1.6}$	$23.69_{0.62}$	$10.81_{0.13}$	$19.57_{0.16}$	$0.824_{0.024}$
350	$567.8_{1.9}$	$18.62_{0.51}$	$8.524_{0.086}$	$20.50_{0.18}$	$0.851_{0.025}$
340	$582.2_{1.1}$	$14.49_{0.38}$	$6.623_{0.060}$	$21.34_{0.13}$	$0.874_{0.024}$
330	$595.8_{1.1}$	$11.15_{0.24}$	$5.061_{0.049}$	$22.112_{0.082}$	$0.895_{0.021}$
320	$610.6_{2.8}$	$8.45_{0.14}$	$3.795_{0.049}$	$22.905_{0.095}$	$0.913_{0.019}$
310	$624.6_{1.8}$	$6.284_{0.087}$	$2.782_{0.051}$	$23.650_{0.059}$	$0.929_{0.021}$

Table SI.XXXVIII: GCMC-MBAR results for 2-butyne with the MiPPE force field. Subscripts correspond to the 95% confidence interval computed with bootstrap re-sampling.

T^{sat} (K)	$\rho_{\mathrm{liq}}^{\mathrm{sat}}$ (kg/m^3)	$\rho_{\mathrm{vap}}^{\mathrm{sat}}$ (kg/m^3)	$P_{\mathrm{vap}}^{\mathrm{sat}}$ (MPa)	ΔH_{v} (kJ/mol)	$Z_{\mathrm{vap}}^{\mathrm{sat}}$
450	$431.8_{7.4}$	$93.5_{4.3}$	$36.24_{0.50}$	$11.93_{0.26}$	$0.561_{0.027}$
440	$466.0_{5.5}$	$74.1_{3.5}$	$30.73_{0.28}$	$14.00_{0.24}$	$0.613_{0.029}$
430	$491.6_{2.0}$	$59.1_{1.9}$	$25.87_{0.16}$	$15.71_{0.17}$	$0.662_{0.022}$
420	$512.10_{0.77}$	$47.58_{0.69}$	$21.63_{0.14}$	$17.114_{0.094}$	$0.704_{0.011}$
410	$530.5_{1.1}$	$38.42_{0.30}$	$17.95_{0.13}$	$18.346_{0.054}$	$0.7411_{7.7e-3}$
400	$548.28_{0.94}$	$30.99_{0.31}$	$14.76_{0.11}$	$19.487_{0.051}$	$0.7745_{9.6e-3}$
390	$565.05_{0.94}$	$24.89_{0.27}$	$12.013_{0.089}$	$20.533_{0.061}$	$0.805_{0.011}$
380	$580.6_{1.1}$	$19.89_{0.25}$	$9.674_{0.068}$	$21.483_{0.073}$	$0.833_{0.012}$
370	$594.97_{0.83}$	$15.78_{0.25}$	$7.697_{0.050}$	$22.349_{0.074}$	$0.858_{0.014}$
360	$608.65_{0.59}$	$12.41_{0.22}$	$6.041_{0.038}$	$23.157_{0.070}$	$0.880_{0.017}$
350	$621.69_{0.66}$	$9.66_{0.19}$	$4.672_{0.041}$	$23.912_{0.091}$	$0.899_{0.019}$
340	$633.85_{0.59}$	$7.42_{0.16}$	$3.552_{0.052}$	$24.60_{0.12}$	$0.916_{0.024}$
330	$646.13_{0.73}$	$5.62_{0.13}$	$2.651_{0.064}$	$25.26_{0.16}$	$0.930_{0.031}$

Table SI.XXXIX: GCMC-MBAR results for 1-pentyne with the MiPPE force field. Subscripts correspond to the 95% confidence interval computed with bootstrap re-sampling.

T^{sat} (K)	$\rho_{\mathrm{liq}}^{\mathrm{sat}}$ (kg/m^3)	$\rho_{\mathrm{vap}}^{\mathrm{sat}}$ (kg/m^3)	$P_{\mathrm{vap}}^{\mathrm{sat}}$ (MPa)	ΔH_{v} (kJ/mol)	$Z_{\mathrm{vap}}^{\mathrm{sat}}$
450	$433.7_{2.3}$	$85.6_{2.5}$	$27.32_{0.22}$	$13.15_{0.18}$	$0.581_{0.018}$
440	$461.7_{1.7}$	$66.9_{2.0}$	$23.04_{0.15}$	$15.29_{0.18}$	$0.641_{0.020}$
430	$485.2_{1.5}$	$53.1_{1.2}$	$19.32_{0.12}$	$17.06_{0.16}$	$0.693_{0.016}$
420	$505.4_{1.6}$	$42.65_{0.51}$	$16.08_{0.12}$	$18.54_{0.11}$	$0.735_{0.010}$
410	$523.3_{1.4}$	$34.37_{0.30}$	$13.27_{0.10}$	$19.810_{0.078}$	$0.7714_{8.8e-3}$
400	$539.7_{1.2}$	$27.67_{0.31}$	$10.844_{0.077}$	$20.949_{0.055}$	$0.803_{0.011}$
390	$555.3_{1.1}$	$22.17_{0.30}$	$8.770_{0.052}$	$21.998_{0.041}$	$0.831_{0.012}$
380	$570.2_{1.0}$	$17.64_{0.27}$	$7.009_{0.033}$	$22.977_{0.033}$	$0.857_{0.014}$
370	$584.03_{0.90}$	$13.91_{0.25}$	$5.528_{0.028}$	$23.874_{0.050}$	$0.880_{0.016}$
360	$596.86_{0.83}$	$10.86_{0.22}$	$4.300_{0.040}$	$24.697_{0.083}$	$0.901_{0.020}$
350	$609.71_{0.69}$	$8.37_{0.19}$	$3.291_{0.055}$	$25.49_{0.11}$	$0.920_{0.026}$
340	$622.58_{0.99}$	$6.37_{0.15}$	$2.474_{0.070}$	$26.27_{0.13}$	$0.936_{0.035}$

Table SI.XL: GCMC-MBAR results for 2-pentyne with the MiPPE force field. Subscripts correspond to the 95% confidence interval computed with bootstrap re-sampling.

T^{sat} (K)	$\rho_{\mathrm{liq}}^{\mathrm{sat}}$ (kg/m^3)	$\rho_{\mathrm{vap}}^{\mathrm{sat}}$ (kg/m^3)	$P_{\mathrm{vap}}^{\mathrm{sat}}$ (MPa)	ΔH_{v} (kJ/mol)	$Z_{\mathrm{vap}}^{\mathrm{sat}}$
470	$445.8_{3.1}$	$83.4_{6.2}$	$27.7_{1.2}$	$14.09_{0.22}$	$0.578_{0.049}$
460	$473.8_{1.9}$	$65.6_{5.4}$	$23.43_{0.88}$	$16.27_{0.30}$	$0.636_{0.057}$
450	$496.8_{1.0}$	$52.5_{3.7}$	$19.73_{0.64}$	$18.06_{0.28}$	$0.685_{0.053}$
440	$516.64_{0.73}$	$42.4_{2.3}$	$16.50_{0.48}$	$19.56_{0.22}$	$0.725_{0.045}$
430	$534.83_{0.74}$	$34.3_{1.7}$	$13.69_{0.36}$	$20.89_{0.19}$	$0.761_{0.042}$
420	$551.57_{0.81}$	$27.7_{1.4}$	$11.26_{0.25}$	$22.08_{0.19}$	$0.792_{0.044}$
410	$566.89_{0.86}$	$22.3_{1.2}$	$9.17_{0.16}$	$23.16_{0.22}$	$0.821_{0.048}$
400	$581.3_{1.1}$	$17.9_{1.0}$	$7.394_{0.080}$	$24.15_{0.26}$	$0.847_{0.049}$
390	$595.3_{1.6}$	$14.24_{0.71}$	$5.890_{0.039}$	$25.09_{0.28}$	$0.869_{0.043}$
380	$608.6_{1.7}$	$11.23_{0.40}$	$4.631_{0.052}$	$25.95_{0.25}$	$0.889_{0.034}$
370	$621.0_{1.3}$	$8.76_{0.19}$	$3.587_{0.066}$	$26.75_{0.19}$	$0.907_{0.026}$
360	$632.99_{0.96}$	$6.75_{0.16}$	$2.735_{0.069}$	$27.52_{0.12}$	$0.922_{0.031}$
350	$644.7_{1.0}$	$5.12_{0.20}$	$2.049_{0.065}$	$28.249_{0.10}$	$0.937_{0.047}$

Table SI.XLI: GCMC-MBAR results for 1-hexyne with the MiPPE force field. Subscripts correspond to the 95% confidence interval computed with bootstrap re-sampling.

T^{sat} (K)	$\rho_{\mathrm{liq}}^{\mathrm{sat}}$ (kg/m^3)	$\rho_{\mathrm{vap}}^{\mathrm{sat}}$ (kg/m^3)	$P_{\mathrm{vap}}^{\mathrm{sat}}$ (MPa)	ΔH_{v} (kJ/mol)	$Z_{\mathrm{vap}}^{\mathrm{sat}}$
490	$423.3_{3.5}$	$87.3_{2.1}$	$25.38_{0.68}$	$14.25_{0.14}$	$0.586_{0.021}$
480	$453.3_{2.0}$	$69.9_{1.5}$	$21.70_{0.60}$	$16.54_{0.12}$	$0.639_{0.022}$
470	$477.4_{1.3}$	$56.51_{0.96}$	$18.44_{0.56}$	$18.448_{0.089}$	$0.686_{0.024}$
460	$497.3_{1.4}$	$46.06_{0.95}$	$15.56_{0.51}$	$20.041_{0.074}$	$0.726_{0.028}$
450	$514.8_{1.3}$	$37.6_{1.3}$	$13.04_{0.44}$	$21.428_{0.10}$	$0.761_{0.037}$
440	$531.5_{1.2}$	$30.7_{1.7}$	$10.84_{0.35}$	$22.71_{0.16}$	$0.792_{0.050}$
430	$547.4_{1.2}$	$25.0_{1.7}$	$8.93_{0.24}$	$23.91_{0.22}$	$0.820_{0.061}$
420	$561.77_{0.87}$	$20.3_{1.5}$	$7.28_{0.13}$	$24.98_{0.23}$	$0.845_{0.063}$
410	$575.17_{0.62}$	$16.34_{0.99}$	$5.875_{0.050}$	$25.97_{0.20}$	$0.867_{0.053}$
400	$588.08_{0.75}$	$13.04_{0.55}$	$4.682_{0.027}$	$26.90_{0.15}$	$0.887_{0.038}$
390	$599.80_{0.63}$	$10.31_{0.28}$	$3.684_{0.047}$	$27.75_{0.11}$	$0.905_{0.027}$
380	$610.32_{0.79}$	$8.06_{0.17}$	$2.858_{0.061}$	$28.507_{0.080}$	$0.922_{0.027}$
370	$621.3_{2.9}$	$6.23_{0.13}$	$2.185_{0.072}$	$29.267_{0.086}$	$0.937_{0.037}$
360	$634.3_{3.1}$	$4.74_{0.11}$	$1.640_{0.083}$	$30.118_{0.078}$	$0.950_{0.053}$

Table SI.XLII: GCMC-MBAR results for 2-hexyne with the MiPPE force field. Subscripts correspond to the 95% confidence interval computed with bootstrap re-sampling.

T^{sat} (K)	$\rho_{\mathrm{liq}}^{\mathrm{sat}}$ (kg/m^3)	$\rho_{\mathrm{vap}}^{\mathrm{sat}}$ (kg/m^3)	$P_{\mathrm{vap}}^{\mathrm{sat}}$ (MPa)	ΔH_{v} (kJ/mol)	$Z_{\mathrm{vap}}^{\mathrm{sat}}$
500	$438.2_{2.9}$	$85.9_{4.0}$	$24.95_{0.26}$	$14.93_{0.36}$	$0.574_{0.027}$
490	$464.9_{1.8}$	$67.7_{2.5}$	$21.31_{0.16}$	$17.31_{0.29}$	$0.635_{0.024}$
480	$486.7_{1.5}$	$54.7_{1.3}$	$18.11_{0.11}$	$19.18_{0.19}$	$0.682_{0.017}$
470	$505.2_{1.7}$	$44.67_{0.74}$	$15.302_{0.087}$	$20.71_{0.14}$	$0.720_{0.013}$
460	$522.5_{2.3}$	$36.61_{0.52}$	$12.839_{0.074}$	$22.09_{0.14}$	$0.753_{0.012}$
450	$539.3_{2.5}$	$29.96_{0.40}$	$10.686_{0.062}$	$23.39_{0.15}$	$0.783_{0.011}$
440	$555.2_{1.8}$	$24.43_{0.31}$	$8.815_{0.050}$	$24.60_{0.11}$	$0.810_{0.011}$
430	$569.62_{0.68}$	$19.82_{0.28}$	$7.201_{0.040}$	$25.678_{0.066}$	$0.835_{0.013}$
420	$583.3_{1.4}$	$15.98_{0.26}$	$5.821_{0.034}$	$26.69_{0.11}$	$0.857_{0.015}$
410	$597.0_{1.4}$	$12.77_{0.22}$	$4.651_{0.035}$	$27.67_{0.12}$	$0.877_{0.017}$
400	$609.9_{1.1}$	$10.11_{0.16}$	$3.669_{0.039}$	$28.59_{0.11}$	$0.896_{0.017}$
390	$621.7_{1.4}$	$7.92_{0.14}$	$2.857_{0.045}$	$29.42_{0.14}$	$0.914_{0.021}$
380	$633.2_{1.2}$	$6.12_{0.16}$	$2.190_{0.050}$	$30.23_{0.16}$	$0.930_{0.032}$
370	$644.01_{0.40}$	$4.67_{0.18}$	$1.653_{0.059}$	$30.98_{0.19}$	$0.944_{0.049}$

Table SI.XLIII: GCMC-MBAR results for 1-heptyne with the MiPPE force field. Subscripts correspond to the 95% confidence interval computed with bootstrap re-sampling.

T^{sat} (K)	$\rho_{\mathrm{liq}}^{\mathrm{sat}}$ (kg/m^3)	$\rho_{\mathrm{vap}}^{\mathrm{sat}}$ (kg/m^3)	$P_{\mathrm{vap}}^{\mathrm{sat}}$ (MPa)	ΔH_{v} (kJ/mol)	$Z_{\mathrm{vap}}^{\mathrm{sat}}$
520	$427.5_{6.0}$	$82.9_{6.4}$	$22.18_{0.71}$	$16.05_{0.64}$	$0.595_{0.050}$
510	$454.3_{2.5}$	$66.9_{4.8}$	$19.06_{0.55}$	$18.37_{0.49}$	$0.646_{0.050}$
500	$476.5_{1.4}$	$54.5_{3.3}$	$16.29_{0.41}$	$20.34_{0.35}$	$0.691_{0.045}$
490	$495.7_{1.4}$	$44.8_{2.4}$	$13.84_{0.30}$	$22.02_{0.25}$	$0.730_{0.042}$
480	$512.9_{1.6}$	$36.9_{1.8}$	$11.68_{0.20}$	$23.51_{0.18}$	$0.764_{0.040}$
470	$528.7_{2.0}$	$30.3_{1.4}$	$9.79_{0.12}$	$24.85_{0.13}$	$0.794_{0.037}$
460	$543.2_{1.9}$	$24.91_{0.95}$	$8.138_{0.072}$	$26.066_{0.092}$	$0.821_{0.032}$
450	$556.9_{1.5}$	$20.37_{0.57}$	$6.705_{0.058}$	$27.199_{0.070}$	$0.846_{0.025}$
440	$570.2_{1.0}$	$16.57_{0.25}$	$5.472_{0.063}$	$28.279_{0.062}$	$0.868_{0.016}$
430	$583.08_{0.58}$	$13.38_{0.11}$	$4.419_{0.062}$	$29.301_{0.062}$	$0.888_{0.015}$
420	$595.19_{0.32}$	$10.71_{0.23}$	$3.526_{0.055}$	$30.253_{0.097}$	$0.907_{0.024}$
410	$606.63_{0.36}$	$8.50_{0.30}$	$2.779_{0.046}$	$31.14_{0.16}$	$0.923_{0.037}$
400	$617.58_{0.39}$	$6.66_{0.33}$	$2.160_{0.048}$	$31.98_{0.23}$	$0.938_{0.050}$
390	$628.63_{0.36}$	$5.16_{0.31}$	$1.654_{0.061}$	$32.81_{0.31}$	$0.950_{0.067}$

Table SI.XLIV: GCMC-MBAR results for 1-octyne with the MiPPE force field. Subscripts correspond to the 95% confidence interval computed with bootstrap re-sampling.

T^{sat} (K)	$\rho_{\mathrm{liq}}^{\mathrm{sat}}$ (kg/m^3)	$\rho_{\mathrm{vap}}^{\mathrm{sat}}$ (kg/m^3)	$P_{\mathrm{vap}}^{\mathrm{sat}}$ (MPa)	ΔH_{v} (kJ/mol)	$Z_{\mathrm{vap}}^{\mathrm{sat}}$
550	$419.4_{3.6}$	$89.5_{1.2}$	$20.75_{0.15}$	$16.27_{0.24}$	$0.5584_{8.6e-3}$
540	$445.2_{3.0}$	$70.95_{0.88}$	$17.88_{0.15}$	$18.98_{0.20}$	$0.6184_{9.2e-3}$
530	$467.6_{2.6}$	$57.19_{0.55}$	$15.35_{0.15}$	$21.30_{0.17}$	$0.6711_{9.1e-3}$
520	$487.1_{2.4}$	$46.85_{0.42}$	$13.11_{0.14}$	$23.22_{0.15}$	$0.7133_{9.8e-3}$
510	$504.3_{2.0}$	$38.69_{0.48}$	$11.14_{0.12}$	$24.87_{0.13}$	$0.748_{0.012}$
500	$519.8_{1.5}$	$32.01_{0.56}$	$9.395_{0.099}$	$26.33_{0.12}$	$0.778_{0.016}$
490	$534.3_{1.2}$	$26.45_{0.57}$	$7.869_{0.075}$	$27.66_{0.13}$	$0.805_{0.019}$
480	$548.2_{1.2}$	$21.77_{0.52}$	$6.539_{0.053}$	$28.92_{0.15}$	$0.829_{0.021}$
470	$561.6_{1.2}$	$17.83_{0.40}$	$5.385_{0.038}$	$30.10_{0.15}$	$0.852_{0.020}$
460	$574.15_{0.95}$	$14.52_{0.26}$	$4.392_{0.033}$	$31.21_{0.13}$	$0.872_{0.017}$
450	$586.02_{0.57}$	$11.73_{0.12}$	$3.546_{0.033}$	$32.245_{0.084}$	$0.890_{0.012}$
440	$597.51_{0.35}$	$9.404_{0.077}$	$2.830_{0.032}$	$33.229_{0.046}$	$0.907_{0.013}$
430	$608.64_{0.40}$	$7.46_{0.15}$	$2.231_{0.029}$	$34.171_{0.089}$	$0.921_{0.022}$
420	$619.31_{0.42}$	$5.86_{0.20}$	$1.736_{0.027}$	$35.06_{0.16}$	$0.935_{0.036}$
410	$630.00_{0.38}$	$4.55_{0.22}$	$1.330_{0.032}$	$35.94_{0.24}$	$0.946_{0.052}$

Table SI.XLV: GCMC-MBAR results for 1-nonyne with the MiPPE force field. Subscripts correspond to the 95% confidence interval computed with bootstrap re-sampling.

T^{sat} (K)	$\rho_{\mathrm{liq}}^{\mathrm{sat}}$ (kg/m^3)	$\rho_{\mathrm{vap}}^{\mathrm{sat}}$ (kg/m^3)	$P_{\mathrm{vap}}^{\mathrm{sat}}$ (MPa)	ΔH_{v} (kJ/mol)	$Z_{\mathrm{vap}}^{\mathrm{sat}}$
570	$427.1_{1.2}$	$80.5_{1.0}$	$17.76_{0.15}$	$18.58_{0.17}$	$0.5782_{8.9e-3}$
560	$450.9_{1.3}$	$64.43_{0.86}$	$15.31_{0.13}$	$21.28_{0.20}$	$0.6340_{9.9e-3}$
550	$471.7_{1.6}$	$52.31_{0.73}$	$13.15_{0.10}$	$23.58_{0.20}$	$0.683_{0.011}$
540	$489.9_{1.5}$	$43.02_{0.62}$	$11.239_{0.080}$	$25.52_{0.17}$	$0.723_{0.012}$
530	$506.3_{1.1}$	$35.61_{0.52}$	$9.552_{0.059}$	$27.21_{0.13}$	$0.756_{0.012}$
520	$521.47_{0.66}$	$29.51_{0.42}$	$8.067_{0.041}$	$28.739_{0.093}$	$0.785_{0.012}$
510	$535.75_{0.67}$	$24.42_{0.33}$	$6.762_{0.026}$	$30.149_{0.083}$	$0.811_{0.012}$
500	$549.10_{0.85}$	$20.14_{0.26}$	$5.626_{0.015}$	$31.452_{0.094}$	$0.835_{0.011}$
490	$561.65_{0.81}$	$16.54_{0.20}$	$4.6410_{9.7e-3}$	$32.666_{0.094}$	$0.856_{0.010}$
480	$573.68_{0.62}$	$13.50_{0.15}$	$3.792_{0.010}$	$33.811_{0.080}$	$0.8746_{9.9e-3}$
470	$585.26_{0.49}$	$10.94_{0.11}$	$3.068_{0.014}$	$34.896_{0.067}$	$0.892_{0.010}$
460	$596.35_{0.58}$	$8.794_{0.096}$	$2.455_{0.017}$	$35.924_{0.069}$	$0.907_{0.012}$
450	$607.27_{0.71}$	$7.003_{0.091}$	$1.942_{0.020}$	$36.924_{0.081}$	$0.921_{0.015}$
440	$618.21_{0.61}$	$5.516_{0.091}$	$1.516_{0.023}$	$37.91_{0.10}$	$0.933_{0.021}$
430	$628.74_{0.51}$	$4.292_{0.090}$	$1.166_{0.026}$	$38.85_{0.14}$	$0.944_{0.029}$
420	$638.50_{0.50}$	$3.296_{0.086}$	$0.885_{0.030}$	$39.72_{0.18}$	$0.955_{0.040}$

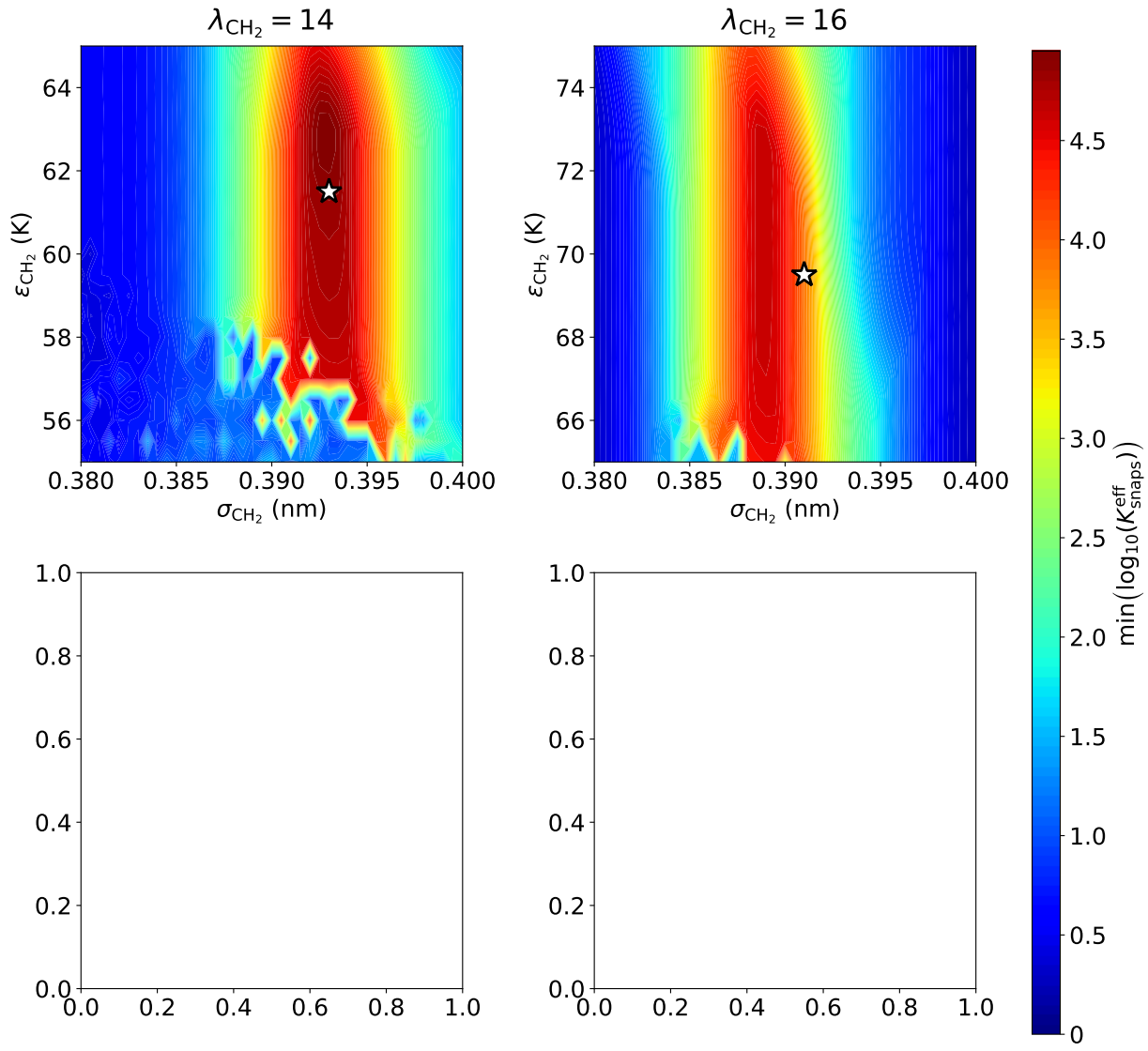

Figure SI.1: Minimum number of effective snapshots $(\min(K^{\text{eff}}_{\text{snaps}}))$ with respect to ϵ_{CH_2} and σ_{CH_2} for cyclohexane. Optimization has converged as $\min(K^{\text{eff}}_{\text{snaps}}) \gg 50$ for the optimal ϵ_{CH_2}, σ_{CH_2}, λ_{CH_2} parameter set. Top-left, top-right, bottom-left, and bottom-right panels correspond $\lambda_{\text{CH}_2} = 14$, $\lambda_{\text{CH}_2} = 16$, $\lambda_{\text{CH}_2} = 18$, and $\lambda_{\text{CH}_2} = 12$, respectively. White star represents the optimal parameter set, i.e., the lowest value of S, for a given λ_{CH_2}